ACS APPLIED MATERIALS & INTERFACES

www.acsami.org

Research Article

Transparent and Sprayable Surface Coatings that Kill Drug-Resistant Bacteria Within Minutes and Inactivate SARS-CoV-2 Virus

Saeed Behzadinasab, Myra D. Williams, Mohsen Hosseini, Leo L. M. Poon, Alex W. H. Chin,* Joseph O. Falkinham, III,* and William A. Ducker*

Cite This: *ACS Appl. Mater. Interfaces* 2021, 13, 54706–54714

Read Online

ACCESS | Metrics & More | Article Recommendations | Supporting Information

ABSTRACT: Antimicrobial coatings are one method to reduce the spread of microbial diseases. Transparent coatings preserve the visual properties of surfaces and are strictly necessary for applications such as antimicrobial cell phone screens. This work describes transparent coatings that inactivate microbes within minutes. The coatings are based on a polydopamine (PDA) adhesive, which has the useful property that the monomer can be sprayed, and then the monomer polymerizes in a conformal film at room temperature. Two coatings are described (1) a coating where PDA is deposited first and then a thin layer of copper is grown on the PDA by electroless deposition (PDA/Cu) and (2) a coating where a suspension of Cu_2O particles in a PDA solution is deposited in a single step (PDA/Cu_2O). In the second coating, PDA menisci bind Cu_2O particles to the solid surface. Both coatings are transparent and are highly efficient in inactivating microbes. PDA/Cu kills >99.99% of *Pseudomonas aeruginosa* and 99.18% of methicillin-resistant *Staphylococcus aureus* (MRSA) in only 10 min and inactivates 99.98% of SARS-CoV-2 virus in 1 h. PDA/Cu_2O kills 99.94% of *P. aeruginosa* and 96.82% of MRSA within 10 min and inactivates 99.88% of SARS-CoV-2 in 1 h.

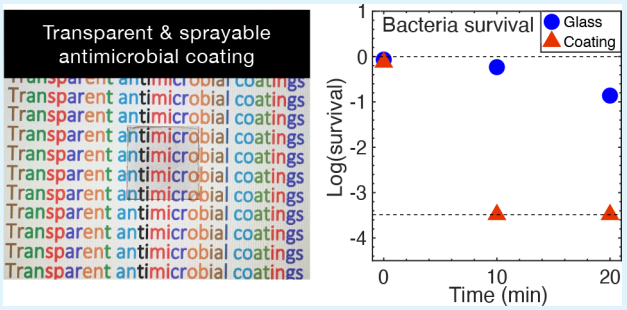

KEYWORDS: *antibacterial, antimicrobial, transparent, coating, drug-resistant bacteria, SARS-CoV-2 virus, COVID-19*

1. INTRODUCTION

Many diseases can spread to humans by fomite transmission.[1] Some of these are bacterial and some are viral. Among bacterial diseases, the ones caused by antibiotic-resistant bacteria are particularly problematic. An example of antibiotic-resistant bacteria is methicillin-resistant *Staphylococcus aureus* (MRSA). MRSA, a Gram-positive bacterium, was declared a "Serious Threat" by the United States Center for Disease Control (CDC) in 2019.[2] It has been the cause of both healthcare-associated infections (HAIs)[3] and community-associated infections (CAIs).[4] MRSA causes a wide range of conditions, such as skin infection, pneumonia, and blood infections.[5,6] *Pseudomonas aeruginosa*, a gram-negative bacterium, is another causative agent of HAIs and has also been labeled by the CDC as a "serious threat".[7] This is one of the more difficult bacteria to kill because it has both intrinsic and acquired resistance to many antibiotics, and it can adapt to the environment to reduce the effectiveness of antibiotics.[8] *P. aeruginosa* causes many diseases, such as blood, lung, or skin infections.[6,9]

Both *P. aeruginosa* and MRSA can survive on solids for a prolonged period of time (even up to months)[10] and are known to be transmitted via direct contact, for example, touching contaminated skins or surfaces.[11,12] To hinder such transmission, it would be desirable to kill the bacteria as soon as they land on surfaces.

The global COVID-19 pandemic has severely impacted life: from early 2020 to July 2021, more than 185 million infections and four million deaths have been attributed to COVID-19,[13] and estimates based on excess deaths suggest that the actual number of deaths may be much higher.[14] The financial cost to the U.S. alone is estimated to be $16 trillion.[15] This disease is caused by the virus known as severe acute respiratory syndrome coronavirus 2 (SARS-CoV-2).

The World Health Organization states that "fomite transmission is considered a likely mode of transmission for SARS-CoV-2".[16] Unpublished experimental work shows that a substantial number of SARS-CoV-2 virus can be transferred to skin from contaminated surfaces.[17] A hamster study found that direct inhalation of infectious droplets is the main mechanism of transmission, but that 1/3 of the animals were infected when exposed to fomites only.[18] Mathematical modeling showed that fomite transmission is responsible for up to 25% of COVID-19 transmission during lockdown.[19]

Received: August 14, 2021
Accepted: October 27, 2021
Published: November 12, 2021

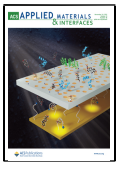

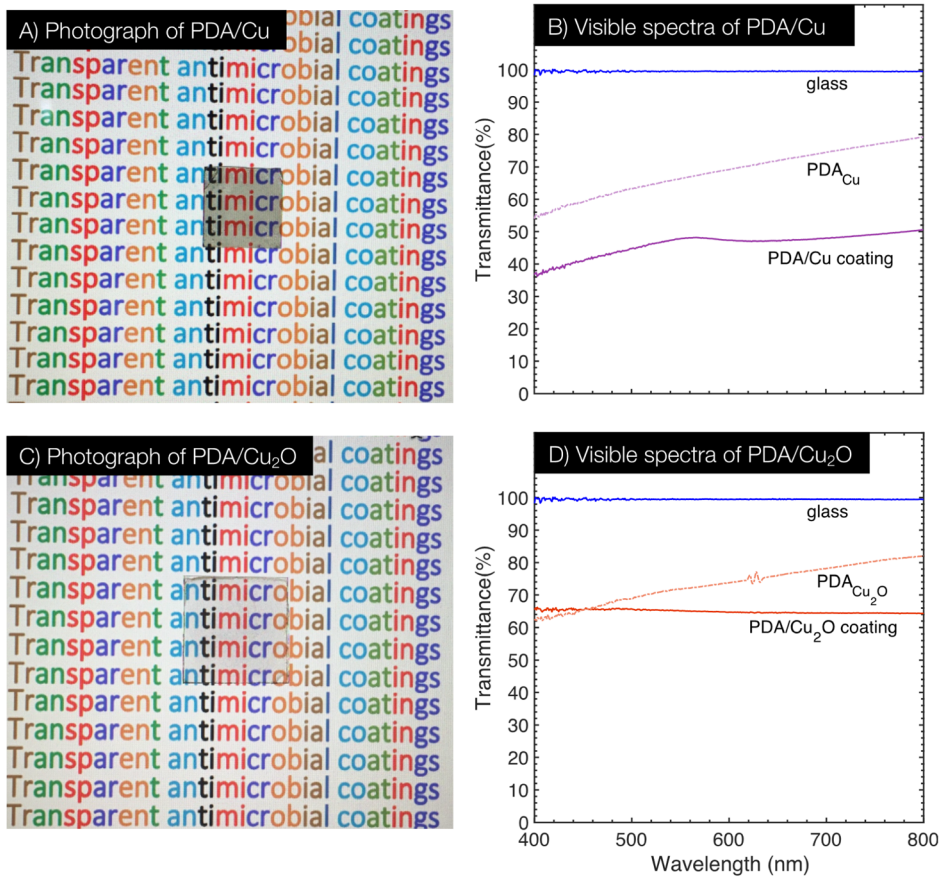

Figure 1. (A,C) photographs of PDA/Cu and PDA/Cu_2O coatings, respectively, held in front of a computer monitor. Both coatings are transparent and allow for all colors to be seen in transmission. (B,D) visible spectra of the coatings. (B) Transmission spectra of PDA, and the PDA/Cu coating. Data for PDA is from the PDA that was prepared in the first step of making the PDA/Cu coating (designated as PDA_{Cu}). (D) Transmission spectra of PDA, and the PDA/Cu coating. The PDA was prepared by the same method as the PDA/Cu_2O coating, but without adding the Cu_2O particles (designated as PDA_{Cu_2O}). The spectra of the two PDAs (i.e., PDA_{Cu} and PDA_{Cu_2O}) are similar. To ensure that coatings formed on one side only for the optical measurements, the PDA_{Cu} and PDA/Cu coatings were prepared with tape covering one side of the glass. The tape was removed prior to spectrometry. The background for the visible spectra is glass.

SARS-CoV-2 also remains infectious up to seven days after a droplet of virus-suspension is placed on solid surfaces.[20,21] The SARS-CoV-2 virus remains infective for up to 9 h (on a dead human skin model[22]) or up to 4 days (on dead pig skin[23]) at room temperature. As a result, there has been significant fear of touching communal objects, and health authorities recommended frequent hand-washing to avoid getting the disease.[24]

The use of common disinfectants, such as 70% ethanol, to decontaminate surfaces is useful for reducing infection, but one significant problem is that contamination can reoccur shortly after the ethanol has evaporated. An alternate approach is to utilize surface coatings that provide an ongoing or continuous kill, and to apply these coatings to everyday solid objects. Some coatings have been developed to meet this objective, both for SARS-CoV-2[25−29] and bacteria,[30,31] and have been reviewed recently.[32−34] In addition, considerable research has investigated the antimicrobial properties of metals and metal oxides,[35−41] textured antimicrobial surfaces,[42−44] and antimicrobial additives to face masks.[45]

An important issue with existing metal and metal oxide coatings is that they are opaque. In some applications this destroys the functionality of the object (e.g., a computer or phone touch screen) and in others, it destroys the aesthetic appeal. To this end, we have developed transparent antimicrobial coatings. To achieve a transparent coating, one needs to avoid both scattering and adsorption of light. Here, we are focused on copper and copper oxides because of their known antimicrobial properties. Bulk copper metal is opaque, but we have used a very thin film to achieve transparency,[46] and electrodeless deposition for ease of use in applications. Cuprous oxide (Cu_2O) is an excellent antimicrobial agent, but it has a red−brown color. For a transparent coating, we simply use a thin, sparse layer of particles. As one decreases the density of particles to obtain transparency, one expects to ultimately lose antimicrobial properties. In fact, we found that a layer that is sufficiently sparse to obtain transparency maintains antimicrobial activity.

We describe two transparent surface coatings that very rapidly inactivate microbes. The adhesive element in the coatings is polydopamine (PDA),[47,48] which polymerizes from aqueous solution at low temperature (<100 °C) in a conformal manner, meaning that PDA takes the shape of the surface. This makes the coatings easy to prepare. Our first coating, designated by PDA/Cu, consists of PDA and a very thin layer of copper that was deposited onto PDA by electroless deposition. Our second coating, designated by PDA/Cu_2O, is made by simultaneously polymerizing PDA and depositing Cu_2O particles in a way that the PDA forms menisci between

https://doi.org/10.1021/acsami.1c15505
ACS Appl. Mater. Interfaces 2021, 13, 54706−54714

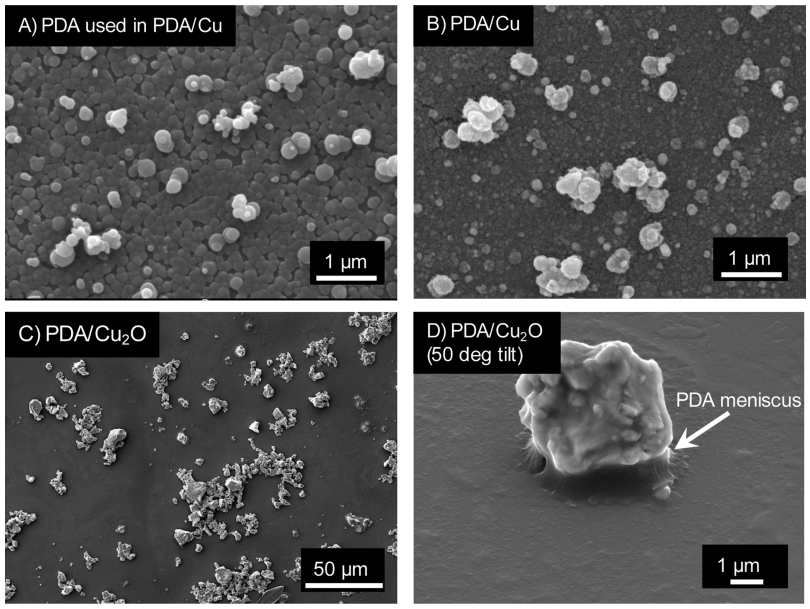

Figure 2. Plan view SEM images of the coatings. (A) PDA-only from an intermediate step in fabrication of the PDA/Cu coating. (B) PDA/Cu coating. The copper coating is apparent from the slight roughening of the coating as well as the filling of depressions compared to A. (C) plan view PDA/Cu_2O coating. (D) 50-degree tilt of magnified view of PDA/Cu_2O coating. The PDA meniscus that holds Cu_2O particles is shown with a white arrow. Further images are shown in Supporting Information Figure S3 and Figure S4.

the Cu_2O particles to hold them on a solid and to bind together the particles. PDA/Cu_2O is sprayable in a single step, which makes it easy and rapid to apply to objects with a variety of shapes. The coatings are thus easy to prepare and also consist of inexpensive and relatively safe materials.

These coatings have an outstanding antimicrobial activity and are transparent. The PDA/Cu coating reduces the number of viable MRSA by 99.18% and the number of viable *P. aeruginosa* by >99.99% compared to uncoated glass within only 10 min. The PDA/Cu_2O coating reduces the number of viable MRSA by 96.82% and the number of viable *P. aeruginosa* by 99.94% compared to uncoated glass within 10 min. The PDA/Cu and PDA/Cu_2O coatings inactivate 99.98 and 99.88%, respectively, of SARS-CoV-2 virus within 1 h, compared to uncoated glass.

2. RESULTS AND DISCUSSION

2.1. Antimicrobial Coatings are Transparent. The antimicrobial coatings are transparent and allow for different colors to be clearly seen when the coatings on glass are held in front of a computer screen. The visible spectra data (Figure 1) confirm that there is little variability for transmission of different colors. The PDA, which forms the basis of both coatings, is already somewhat opaque, absorbing 20−40% of the light. The two coatings were made in different ways so have slightly different transmission. Addition of copper to PDA decreases the transmission, with slightly more adsorption at a longer wavelength as expected,[46] which counteracts the absorption trend for PDA to give a more consistent transmission than PDA alone. The PDA/Cu_2O coating also transmits less light than PDA alone, presumably because of scattering and absorbance by the particles (See Figure S2 for particle size distribution.).

2.2. Other Characterization of the Coatings. For antimicrobial activity, the active ingredients, that is, copper or Cu_2O, should be accessible from the surface, and we verified this with SEM imaging and XPS, which is sensitive to the chemistry in the outer few nanometers of a surface. Considering first the PDA/Cu coating, the copper in the PDA/Cu coating was grown from the surface of a PDA coating. That PDA coating is rough (Figure 2A), by design, to present a large surface area on which Cu can form. After deposition of the Cu, some depressions in the PDA coating have been filled in (see Figure 2) and additional small-scale roughness is visible (see Figure S3E,F in Supporting Information). SEM images show that the copper layer is approximately 22 nm thick and the PDA is about 55 nm thick (see Figure S3E,F). The presence of Cu in the PDA/Cu coating is also obvious from XPS: the PDA/Cu coating is about 37% copper (see Figure S5 in Supporting Information for XPS spectra). High resolution XPS (Figure S5) is consistent with an oxidized outer layer consisting of both Cu(I) and Cu(II) species, as observed previously.[49,50] Consistent with the existing literature on electroless deposition,[47,51−54] in this paper, we will refer to the coating as copper or Cu, even though the oxidation state of the inner part of the 22 nm layer film is not clear from the XPS spectra (see Figure S6).

The PDA/Cu_2O coating utilizes Cu_2O particles that have a mean size of about 5 μm (see Figure S2 for Cu_2O particles size distribution), which is a much larger scale than the thickness of the Cu coating in the PDA/Cu coating. In the preparation of the PDA/Cu_2O coating, we incorporated a heat treatment step at 80 °C for 30 min. XPS shows that both Cu(I) and Cu(II) are present on the outer 1 nm or so of the coating (see Figure S5). However, the duration and temperature of heat-treatment is not sufficient to oxidize Cu_2O, consistent with our previous work.[25]

The Cu_2O particles clearly protrude from the PDA (Figure 2D). Our goal was a coating with good transparency, so knowing that the Cu_2O particles scatter light, we have deliberately made a sparse layer of Cu_2O (Figure 2C,D). XPS data show that the PDA/Cu_2O coating contains only 5.7% percent copper (see Figure S5 in Supporting

https://doi.org/10.1021/acsami.1c15505
ACS Appl. Mater. Interfaces 2021, 13, 54706−54714

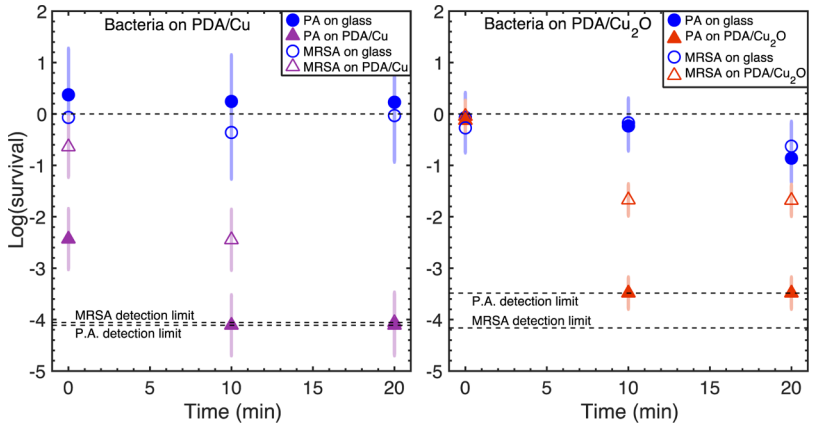

Figure 3. Time course of survival of *P. aeruginosa* (PA) and methicillin-resistant *S. aureus* (MRSA) on transparent PDA/Cu (left) and PDA/Cu_2O (right) coatings. Survival was calculated with eq 3, so zero represents the CFU in the initial droplet. For the coatings, each symbol represents the average of three separate samples, the error bar is the comparison interval from ANOVA, and the detection limit for each bacterium is shown with a dotted line. Compared to the glass control, within 10 min, the PDA/Cu coating caused a reduction of more than 99.99% of *P. aeruginosa* and 99.18% of MRSA, and the PDA/Cu_2O caused a reduction of more than 99.94% of *P. aeruginosa* and 96.82% of MRSA. We performed a three-way ANOVA with each of the coatings: factor 1 = surface type (glass vs each coating), factor 2 = time, factor 3 = bacteria type (*P. aeruginosa* and MRSA). The *p*-values for surface type were $<10^{-10}$ for PDA/Cu and $<10^{-9}$ for PDA/Cu_2O. Each data point is tabulated in Supporting Information.

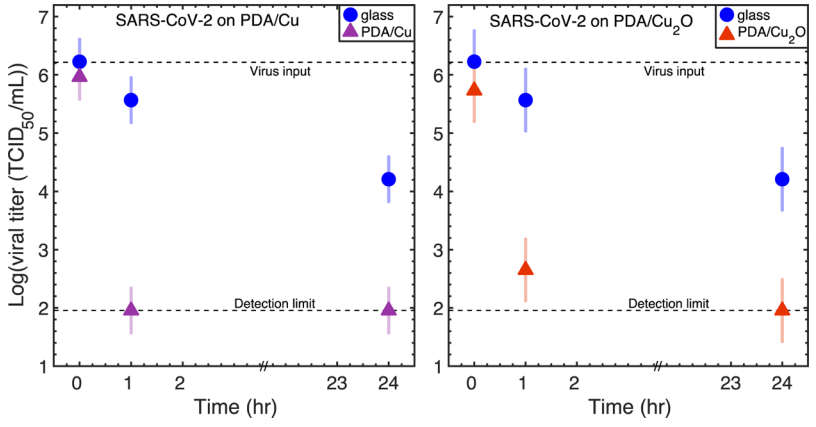

Figure 4. Time course of SARS-CoV-2 titer for transparent PDA/Cu (left) and PDA/Cu_2O (right) coatings. Each marker shows the average of three independent samples and the error bars are the comparison interval from ANOVA. The detection limit was 90 TCID50/mL (shown with dotted line). When data were below the detection limit, the point was plotted at the detection limit. PDA/Cu reduces the infectivity of SARS-CoV-2 by 99.98% and PDA/Cu_2O reduces the infectivity by 99.88% in 1 h. We performed a 2-way ANOVA with each of the coatings: factor 1 = surface type (glass vs each coating), factor 2 = time. The *p*-value for coating was $<10^{-8}$ for PDA/Cu and $<10^{-6}$ for PDA/Cu_2O. Each data point is tabulated in Supporting Information, Table S6.

Information). Closer inspection of the SEM image that was taken on a tilt angle reveals the formation of a PDA meniscus that helps to adhere the Cu_2O particles to the substrate.

Advancing and receding water contact angles for PDA/Cu are 72 ± 22 and 10 ± 7° (the number after "±" sign is the 95% confidence interval from measurements of independent samples). The PDA/Cu_2O is hydrophilic, with both advancing and receding angles being <10°.

2.3. Inactivation of Microbes. *2.3.1. Both Transparent Coatings Kill Bacteria in 10 Min.* Figure 3 shows very low survival of *P. aeruginosa* and MRSA on each of the transparent coatings, even after only 10 min. Survival is a comparison between the input titer and the titer at a later time and is calculated from

$$\log \text{survival} = \text{mean}\left[\log_{10}\left(\frac{\text{sample titer}}{\text{units}}\right)\right] - \text{mean}\left[\log_{10}\left(\frac{\text{input titer}}{\text{units}}\right)\right] \quad (1)$$

$$\%\ \text{survival} = [1 - 10^{-\log \text{survival}}] \times 100 \quad (2)$$

Microbes can become inactivated with time on inanimate surfaces, and bacteria can die, even without an active ingredient, so we also measured survival of the microbes on the uncoated glass as a control. Figure 3 shows that survival is very high on uncoated glass. Our performance metric is "reduction", which is a comparison of the titer on the coated and uncoated samples

https://doi.org/10.1021/acsami.1c15505
ACS Appl. Mater. Interfaces 2021, 13, 54706−54714

$$\text{log reduction} = \text{mean}\left[\log_{10}\left(\frac{\text{uncoated glass titer}}{\text{units}}\right)\right] - \text{mean}\left[\log_{10}\left(\frac{\text{sample titer}}{\text{units}}\right)\right] \quad (3)$$

$$\%\ \text{reduction} = [1 - 10^{-\log\ \text{reduction}}] \times 100 \quad (4)$$

The % reduction by PDA/Cu is 99.99% (4-logs) for *P. aeruginosa* and 99.18% (>2-logs) for MRSA within only 10 min (Figure 3). The reduction on PDA/Cu_2O is 99.94% (>3-logs) for *P. aeruginosa* and 96.82% (~2-logs) for MRSA in 10 min. This compares favorably to the typical United States Environmental Protection Agency (EPA) standards of 99.9% (3-logs) in 1 h of exposure.[55]

We also measured antimicrobial properties of PDA alone and found that PDA did not have antimicrobial activity against bacteria or viruses (see Supporting Information, Figures S7 and S8), confirming that copper and Cu_2O are the active ingredients in the two coatings.

2.3.2. Both Coatings Rapidly Inactivate SARS-CoV-2. PDA/Cu and PDA/Cu_2O coatings reduce the infectivity of SARS-CoV-2 virus by 99.98 and 99.88% within 1 h, respectively compared to a glass control (see Figure 4). PDA alone does not inactivate SARS-CoV-2 (see Figure S8), demonstrating that the Cu and Cu_2O are the active ingredients.

The PDA/Cu_2O results can be compared to our previous results for Cu_2O in a polyurethane coating.[25] The earlier coating used a much higher loading of Cu_2O particles, such that the coating was completely opaque, and it inactivated ~99.9% of SARS-CoV-2 after 1 h. The similarity of the results for the two coatings shows that there is little benefit to the greater solids loading. On the other hand, the lower solids loading confers the significant advantage that the coating is transparent and therefore can be used on touch screens, monitors, and so forth, and maintains aesthetic appeal of solids. Additionally, the similarity of two results supports the idea that the killing is a surface effect. The infectivity of SARS-CoV-2 over time was previously measured on a copper sheet. In that work, the virus remained infectious for 4−8 h,[20] while here, ~99.9% of it is inactivated within 1 h on our coatings. Note that in the work on copper,[20] the starting titer was about log(TCID50/mL) of 3.7, which is about 2.5 logs lower that in this work. The coatings therefore work more rapidly than copper, even with a greater initial dose of virus.

2.4. Mechanism of Action. The mechanism of action of copper or Cu_2O against microbes is one or combination of three routes: contact killing, ion release, and generation of reactive oxygen species (ROSs).[32,35,56] In the contact killing route, the microbe needs to physically make contact with the active ingredient. Ion release from copper can be in the forms of simple ions (Cu^+ and Cu^{2+}),[35] and possibly hydroxides and/or oxides of copper ions[57] where the composition of copper species depends on the presence of other ions.[58] These dissolved species are typically cationic and can interact with anionic biomolecules such as DNA,[59] RNA, some lipids, parts of proteins, and so forth. For example, copper species may inactivate metalloenzymes by replacing native metal ions.[32] Another mechanism is that Cu_2O is thought to produce ROSs, including superoxide ($O_2^{-\bullet}$), hydroxyl radicals (•OH), and hydrogen peroxide (H_2O_2), which can oxidize biological materials.[35] Typically, this oxidation begins with superoxide and/or hydrogen peroxide, which are produced by bacteria but not viruses. The current literature appears to propose that the generation of ROSs does not play a role in inactivation of viruses.[35,60]

2.5. PDA/Cu_2O Coating is Sprayable. It is desirable that a coating is easy to deploy, and spraying is one of the fastest techniques for coating. The microbial results above are for drop-casted coatings. We made a second set of PDA/Cu_2O coatings by spraying glass with a suspension of Cu_2O suspension in aqueous dopamine (see Experimental Section), and subsequently dried the coated slides at 80 °C in an oven. The sprayed coating was characterized with UV−Vis, SEM, and XPS (see Figure S9 in Supporting Information). The results were similar to the drop-cast coating, that is, the coating was transparent with wavelength-independent transmission (Figure S9D), XPS shows a similar copper composition and SEM shows that the particles protrude from the PDA.

Spraying was typically performed within about 4−5 min after the suspension was prepared. At this time, the particles were still suspended. We found that the particles eventually sedimented, but after sedimentation, the particles could be resuspended simply by shaking and then sprayed.

2.6. Other Aspects of the Coatings. The polymerization of dopamine is achieved in water, which is an environmental-friendly and non-toxic solvent. Likewise, PDA is non-toxic: PDA nanoparticles injected in a mice have a median lethal dose (LD_{50}) in the range 400−585 mg/kg.[61] Although copper has some toxicity to aquatic species, the US EPA allows for its use in antimicrobial coatings.[62] Also, since ancient times, copper has been in wide circulation as coins that are already frequently handled by the public. The cost of copper in 2021 is about $6 per kg, which is not a substantial factor in a coating that is very thin. In some applications, surfaces are wiped periodically with disinfectant. We tested the antimicrobial efficacy of the coating after it was abraded by a sponge that was wetted with 70% ethanol, and found that the coating still caused a reduction of ~99.8% (see Table S1). Finally, the process of coating is simple, using spraying or dip coating, with low temperature curing, and no need for expensive equipment.

3. CONCLUSIONS

Two methods are described for rapidly preparing transparent antimicrobial coatings based on PDA using inexpensive and relatively safe materials. These coatings are very effective at both killing bacteria and inactivating the SARS-CoV-2 virus. Using a thin layer of copper deposited on a PDA layer, we achieved a reduction of >99.99% of *P. aeruginosa* and 99.18% of MRSA within 10 min compared to a glass control, as well as 99.98% reduction of SARS-CoV-2 virus infectivity in 1 h. Using a sparse layer of Cu_2O bound to, but protruding from PDA, we obtained a reduction of 99.94% of *P. aeruginosa* and 96.82% of MRSA within 10 min, as well as 99.88% of SARS-CoV-2 virus in 1 h compared to a glass control. The activity against SARS-CoV-2 virus is similar to the activity obtained from much greater solids loading in previous work. The coatings are thus highly effective against important pathogens and should find applications on common-use objects to reduce the spread of microbial diseases. A transparent coating is an essential feature for a coating on touch screens, and also extremely desirable for maintaining the visual appeal of an object while achieving a strong antimicrobial effect.

https://doi.org/10.1021/acsami.1c15505
ACS Appl. Mater. Interfaces 2021, 13, 54706−54714

4. EXPERIMENTAL SECTION

4.1. Materials. Glass slides (25 × 75 × 1 mm), 200 Proof ethanol, 70% ethanol, nitric acid (70%, ACS grade) and sodium hydroxide (beads, ACS grade) were purchased from VWR. The following were purchased from Fischer Scientific: dopamine hydrochloride (99%) and dimethylamineborane (DMAB, 98%). Cu_2O particles (Chem Copp HP III UltraFine Type -5; mean size = 5.4 μm) were purchased from American Chemet Corporation. The following were obtained from Sigma Aldrich: copper(II) chloride (97%), boric acid (ACS reagent), tris(hydroxymethyl)aminomethane (Tris, ACS reagent), and ethylenediaminetetraacetic acid (EDTA, >99%). Tryptic soy broth (TSB) and tryptic soy agar (TSA) were purchased from BD, Sparks, MD. Cell suspensions were diluted in either phosphate-buffered saline (PBS) or DE Broth (BD, Sparks, MD). Water was purified by Milli-Q Reference system. Glass slides were serially cleaned with DI water, 70% ethanol, DI water, nitric acid (6 M), and DI water, and subsequently dried with high pressure nitrogen.

4.2. Fabrication of the Surface Coatings. *4.2.1. Fabrication of PDA/Cu Coating.* A two-step procedure was used in which the first step was coating preparation of a thin coating of PDA.[47,63] Pieces of cleaned glass slides (12 × 12 mm) were immersed in tris solution (10 mM in water) at 60 °C and stirred. Dopamine hydrochloride was added to achieve a final concentration of 5 g dopamine/L and then stirring at 60 °C continued for 4 h. After cooling to room temperature, the glass slides were washed with purified water and dried with nitrogen gas. PDA makes conformal coatings on solids, so we assume that the coating forms on both sides of the glass,[47] but we always tested the coating on the side that was not touching the container. Copper was deposited onto a preformed layer of PDA, using a method from the literature,[47,51−54] but with a thinner layer than in previous work. The copper was electrolessly deposited using an aqueous solution containing EDTA (50 mM), $CuCl_2$ (50 mM), and boric acid (100 mM) with the pH adjusted to 7 using NaOH solution.[47,51−54] The solution was placed on a heater at 37 °C under stirring. DMAB was added to achieve a final concentration of 100 mM and subsequently, PDA-coated glass-slides were immersed in the solution. The reaction was stopped 30 min after the solution color changed to dark green. The samples were washed with DI water and dried with high-pressure nitrogen.

4.2.2. Fabrication of PDA/Cu_2O Coating. A 0.2% w/w suspension of Cu_2O particles in tris solution (10 mM) was sonicated for 1 h. Dopamine hydrochloride was added to achieve a concentration of 0.05 g dopamine/L. Next, 140 μL of Cu_2O and dopamine suspension was drop cast on 15 × 15 mm pieces of cleaned glass slides, to give a Cu_2O-loading of 1.27×10^{-4} g/cm^2. Two to 3 min after deposition, the samples were heat-treated at 80 °C in an oven for 30 min to dry. Subsequently, they were forcefully blown with high pressure nitrogen gas. These samples were coated on one side of the glass only.

4.3. Characterization. SEM (JEOL IT500) was used to characterize the morphology of the coatings (the samples were coated with 5 nm of Pt/Pd prior to SEM measurements). XPS (PHI VersaProbe III with a monochromatic Al Kα source of 1486.6 eV) was utilized for measuring of chemical composition of the samples. UV−Vis transmittance was measured using an Agilent model 8453 UV-VIS spectrometer. Water contact angles were measured using First Ten Angstroms FTA125.

4.4. Antibacterial Assay. *4.4.1. Microbial Strains.* The microbial strains employed in this study were *P. aeruginosa* strain (DSM-9644) and methicillin-resistant *S. aureus* (MRSA) strain (MA43300, obtained from the Danville Community Hospital, VA).

4.4.2. Growth of Microbial Strains. Each bacterial strain was grown in 5 mL of TSB (BD, Sparks, MD) to mid-exponential phase at 37 °C with aeration (60 rpm). Following growth, the purity and identity of the cells in the cultures were verified by streaking bacterial cultures on TSA (BD, Sparks, MD) and incubated at 37 °C for 48 h and examining colonies for species-specific traits (e.g., pigmentation and surface texture).

4.4.3. Preparation of Microbial Strains for Testing. Grown cells were collected by centrifugation (5000*g* for 20 min), the supernatant medium discarded, and the cells were resuspended in 5 mL of sterile phosphate-buffered saline (PBS) by vortexing for 60 s. Those suspensions were centrifuged (5000*g* for 20 min), the supernatant was discarded, and the washed cells suspended in 5 mL of sterile PBS by vortexing for 60 s. The number of colony-forming units (CFU)/mL of each washed suspension was measured by spreading 0.10 mL (in duplicate) of serial dilutions in PBS on TSA plates.

4.4.4. Measurement of Cell Number. The cell number of PBS-suspensions of bacteria were measured as colony-forming units (CFU)/mL of suspension. A 10-fold dilution series was prepared for each suspension in either PBS or DE Broth, 0.1 mL of each dilutions was spread on TSA in triplicate, and colonies were counted after 48 h incubation at 37 °C. If zero colonies were present for the least dilution, then to enable a log transformation of all data, we designated the zero as one. This is the detection limit, which is an upper bound.

4.4.5. Measurement of Surface-Killing. For each microbial strain, a 5 μL droplet of bacterial cells in PBS was placed on each coated or uncoated glass sample. Immediately and after 10 and 20 min (or longer where noted), each sample was transferred to a separate sterile 50 mL centrifuge tube containing 5 mL of PBS or DE broth, vortexed at the highest setting for 10 s and sonicated for 1 min in a Branson model 12 Ultrasonic Cleaner (Shelton, CT) to detach cells from the solid, and then the CFU/mL of the resulting bacterial suspension measured by removing a sample of the suspension without coming in contact with the glass sample and preparing a dilution series. The process was repeated at each time point, and three different samples were used for each condition, that is, each surface coating at each time. Note that the bacterial suspension contacts only one side of the glass.

4.5. SARS-CoV-2 Assay. The viral assay methods were described previously.[25,27] In summary, the stock virus (BetaCoV/Hong Kong/VM20001061/2020, isolated from a confirmed COVID-19 patient in Hong Kong) was prepared in Vero-E6 cells cultured in Dulbecco's Modified Eagle Medium with 2% fetal bovine serum and 1% v/v penicillin−streptomycin at 37 °C with 5% CO_2. Prior to tests with the virus, all of the surfaces were sterilized with 70% ethanol and air-dried. A 5 μL SARS-CoV-2 droplet at 7.8 $\log_{10}$ unit $TCID_{50}$/mL was placed on the test solid (temp = 22−23 °C and 60−70% relative humidity) and after a prescribed time, the solid was soaked in 300 μL of viral transport medium [Earle's balanced salt solution including 0.5% (w/v) bovine serum albumin and 0.1% (w/v) glucose, pH 7.4] to elute the virus. Subsequently, the eluted virus was titrated by 50% tissue culture infective dose ($TCID_{50}$) assay in Vero E6 cells.[64,65] In brief, confluent Vero E6 cells on 96-well plates were infected with serially diluted virus in quadruplicates. The infected cells were incubated at 37 °C with 5% CO_2. On day 5 post-infection, the cells were examined for a cytopathic effect. The $TCID_{50}$/mL is the dilution that caused a cytopathic effect in 50% of treated Vero E6 cell cultures. Three independent samples were tested at each condition.

4.6. Calculation of Microbe Survival and Reduction. Microbe survival and reduction are defined in eqs 1−4. We use the word survival for simplicity but acknowledge that the CFU assay measures those cells that can reproduce to form a colony and that the $TCID_{50}$ assay does not measure numbers of virions.

4.7. Statistical Analysis. The statistical analysis used N-way ANOVA in MATLAB. The error bars were calculated for each figure with Post Hoc multiple comparison using Dunn-Sidák's approach. We chose a significance level of 0.05. Before statistical analysis, each microbial titer was $\log_{10}$ transformed.

DATA AVAILABILITY STATEMENT

The raw data that support the findings of this study are available in the Supporting Information file.

ASSOCIATED CONTENT

Supporting Information

The Supporting Information is available free of charge at https://pubs.acs.org/doi/10.1021/acsami.1c15505.

https://doi.org/10.1021/acsami.1c15505
ACS Appl. Mater. Interfaces 2021, 13, 54706−54714

Schematic of abrasion tests, particle Size Distribution of Cu_2O particles, additional SEM images of PDA (prior to copper deposition) and PDA/Cu, additional SEM images of coatings, XPS results, XPS results of Ar^+-etched coatings, bacteria assay for PDA sample, SARS-CoV-2 titer for PDA sample, characterization of PDA/Cu_2O coating on glass that was prepared by spray-coating, data tables (PDF)

AUTHOR INFORMATION

Corresponding Authors

Alex W. H. Chin − *School of Public Health, LKS Faculty of Medicine, The University of Hong Kong, Hong Kong, China; Centre for Immunity and Infection, Hong Kong Science Park, Hong Kong, China;* orcid.org/0000-0002-6556-9092; Email: alexchin@hku.hk

Joseph O. Falkinham, III − *Department of Biological Sciences, Virginia Tech, Blacksburg, Virginia 24061, United States;* Email: jofiii@vt.edu

William A. Ducker − *Department of Chemical Engineering and Center for Soft Matter and Biological Physics, Virginia Tech, Blacksburg, Virginia 24061, United States;* orcid.org/0000-0002-8207-768X; Email: wducker@vt.edu

Authors

Saeed Behzadinasab − *Department of Chemical Engineering and Center for Soft Matter and Biological Physics, Virginia Tech, Blacksburg, Virginia 24061, United States;* orcid.org/0000-0002-6271-2623

Myra D. Williams − *Department of Biological Sciences, Virginia Tech, Blacksburg, Virginia 24061, United States*

Mohsen Hosseini − *Department of Chemical Engineering and Center for Soft Matter and Biological Physics, Virginia Tech, Blacksburg, Virginia 24061, United States*

Leo L. M. Poon − *School of Public Health, LKS Faculty of Medicine and HKU-Pasteur Research Pole, LKS Faculty of Medicine, The University of Hong Kong, Hong Kong, China; Centre for Immunity and Infection, Hong Kong Science Park, Hong Kong, China*

Complete contact information is available at: https://pubs.acs.org/10.1021/acsami.1c15505

Notes

The authors declare the following competing financial interest(s): WD declares part ownership in a startup company that intends to produce surface coatings. Other authors declare no conflict of interest.

ACKNOWLEDGMENTS

This work was supported by the National Science Foundation (NSF) under Grant no. CBET-1902364, the Health and Medical Research Fund (COVID190116), and the National Institute of Allergy and Infectious Diseases (contract HHSN272201400006C). This work used shared facilities at the Virginia Tech National Center for Earth and Environmental Nanotechnology Infrastructure supported by NSF (ECCS 1542100 and ECCS 2025151). We also thank Dr. Xu Feng, who captured the XPS spectra and provided analysis, and the Surface Analysis Laboratory in the Department of Chemistry at VT, which is supported by the NSF under Grant no. CHE-1531834.

REFERENCES

(1) Stephens, B.; Azimi, P.; Thoemmes, M. S.; Heidarinejad, M.; Allen, J. G.; Gilbert, J. A. Microbial Exchange Via Fomites and Implications for Human Health. *Curr. Pollut. Rep.* **2019**, *5*, 198−213.

(2) Centers for Disease Control and Prevention Methicillin-Resistant Staphylococcus Aureus (Mrsa). https://www.cdc.gov/drugresistance/pdf/threats-report/mrsa-508.pdf (accessed June 2, 2021).

(3) Maree, C. L.; Daum, R. S.; Boyle-Vavra, S.; Matayoshi, K.; Miller, L. G. Community-associated Methicillin-resistantStaphylococcus aureusIsolates and Healthcare-Associated Infections1. *Emerg. Infect. Dis.* **2007**, *13*, 236.

(4) David, M. Z.; Daum, R. S. Community-Associated Methicillin-Resistant Staphylococcus aureus : Epidemiology and Clinical Consequences of an Emerging Epidemic. *Clin. Microbiol. Rev.* **2010**, *23*, 616−687.

(5) Pantosti, A.; Venditti, M. What Is Mrsa? *Eur. Respir. J.* **2009**, *34*, 1190−1196.

(6) Williams, B. J.; Dehnbostel, J.; Blackwell, T. S. Pseudomonas Aeruginosa: Host Defence in Lung Diseases. *Respirology* **2010**, *15*, 1037−1056.

(7) Centers for Disease Control and Prevention Multidrug-Resistant Pseudomonas Aeruginosa https://www.cdc.gov/drugresistance/pdf/threats-report/pseudomonas-aeruginosa-508.pdf (accessed June 2, 2021).

(8) Pang, Z.; Raudonis, R.; Glick, B. R.; Lin, T.-J.; Cheng, Z. Antibiotic Resistance in Pseudomonas Aeruginosa: Mechanisms and Alternative Therapeutic Strategies. *Biotechnol. Adv.* **2019**, *37*, 177−192.

(9) Campa, M.; Bendinelli, M.; Friedman, H. *Pseudomonas Aeruginosa as an Opportunistic Pathogen*; Springer Science & Business Media: New York, NY, 1993.

(10) Kramer, A.; Schwebke, I.; Kampf, G. How Long Do Nosocomial Pathogens Persist on Inanimate Surfaces? A Systematic Review. *BMC Infect. Dis.* **2006**, *6*, 130.

(11) Vos, M. C.; Verbrugh, H. A. Mrsa: We Can Overcome, but Who Will Lead the Battle? *Infect. Control Hosp. Epidemiol.* **2005**, *26*, 117−120.

(12) de Abreu, P. M.; Farias, P. G.; Paiva, G. S.; Almeida, A. M.; Morais, P. V. Persistence of Microbial Communities Including Pseudomonas Aeruginosa in a Hospital Environment: A Potential Health Hazard. *BMC Microbiol.* **2014**, *14*, 118.

(13) World Health Organization. Who Coronavirus Disease (Covid-19) Dashboard. https://covid19.who.int/ (accessed July 7th, 2021).

(14) IHME Estimation of Total Mortality Due to Covid-19. http://www.healthdata.org/special-analysis/estimation-excess-mortality-due-covid-19-and-scalars-reported-covid-19-deaths (accessed May 13, 2021).

(15) Cutler, D. M.; Summers, L. H. The Covid-19 Pandemic and the $16 Trillion Virus. *JAMA* **2020**, *324*, 1495−1496.

(16) World Health Organization. Transmission of Sars-Cov-2: Implications for Infection Prevention Precautions. https://www.who.int/news-room/commentaries/detail/transmission-of-sars-cov-2-implications-for-infection-prevention-precautions (accessed Feb 28, 2021).

(17) Behzadinasab, S.; Chin, A. W. H.; Hosseini, M.; Poon, L. L. M.; Ducker, W. A. Sars-Cov-2 Virus Transfers to Skin through Contact with Contaminated Solids. medRxiv: 2021.04.24.21256044 **2021**.

(18) Sia, S. F.; Yan, L.-M.; Chin, A. W. H.; Fung, K.; Choy, K.-T.; Wong, A. Y. L.; Kaewpreedee, P.; Perera, R. A. P. M.; Poon, L. L. M.; Nicholls, J. M.; Peiris, M.; Yen, H.-L. Pathogenesis and Transmission of Sars-Cov-2 in Golden Hamsters. *Nature* **2020**, *583*, 834−838.

(19) Meiksin, A. Dynamics of Covid-19 Transmission Including Indirect Transmission Mechanisms: A Mathematical Analysis. *Epidemiol. Infect.* **2020**, *148*, No. e257.

(20) Van Doremalen, N.; Bushmaker, T.; Morris, D. H.; Holbrook, M. G.; Gamble, A.; Williamson, B. N.; Tamin, A.; Harcourt, J. L.; Thornburg, N. J.; Gerber, S. I.; Lloyd-Smith, J. O.; de Wit, E.;

Munster, V. J. Aerosol and Surface Stability of Sars-Cov-2 as Compared with Sars-Cov-1. *N. Engl. J. Med.* **2020**, *382*, 1564−1567.
(21) Chin, A. W. H.; Chu, J. T. S.; Perera, M. R. A.; Hui, K. P. Y.; Yen, H.-L.; Chan, M. C. W.; Peiris, M.; Poon, L. L. M. Stability of Sars-Cov-2 in Different Environmental Conditions. *Lancet Microbe* **2020**, *1*, No. e10.
(22) Hirose, R.; Ikegaya, H.; Naito, Y.; Watanabe, N.; Yoshida, T.; Bandou, R.; Daidoji, T.; Itoh, Y.; Nakaya, T. Survival of Severe Acute Respiratory Syndrome Coronavirus 2 (Sars-Cov-2) and Influenza Virus on Human Skin: Importance of Hand Hygiene in Coronavirus Disease 2019 (Covid-19). *Clin. Infect. Dis.* **2020**, ciaa1517.
(23) Harbourt, D. E.; Haddow, A. D.; Piper, A. E.; Bloomfield, H.; Kearney, B. J.; Fetterer, D.; Gibson, K.; Minogue, T. Modeling the Stability of Severe Acute Respiratory Syndrome Coronavirus 2 (Sars-Cov-2) on Skin, Currency, and Clothing. *PLoS Neglected Trop. Dis.* **2020**, *14*, No. e0008831.
(24) Alzyood, M.; Jackson, D.; Aveyard, H.; Brooke, J. COVID-19 reinforces the importance of handwashing. *J. Clin. Nurs.* **2020**, *29*, 2760−2761.
(25) Behzadinasab, S.; Chin, A.; Hosseini, M.; Poon, L.; Ducker, W. A. A Surface Coating That Rapidly Inactivates Sars-Cov-2. *ACS Appl. Mater. Interfaces* **2020**, *12*, 34723−34727.
(26) Hutasoit, N.; Kennedy, B.; Hamilton, S.; Luttick, A.; Rahman Rashid, R. A.; Palanisamy, S. Sars-Cov-2 (Covid-19) Inactivation Capability of Copper-Coated Touch Surface Fabricated by Cold-Spray Technology. *Manuf. Lett.* **2020**, *25*, 93−97.
(27) Hosseini, M.; Chin, A. W. H.; Behzadinasab, S.; Poon, L. L. M.; Ducker, W. A. Cupric Oxide Coating That Rapidly Reduces Infection by Sars-Cov-2 Via Solids. *ACS Appl. Mater. Interfaces* **2021**, *13*, 5919−5928.
(28) Sousa, B. C.; Cote, D. L. Antimicrobial Copper Cold Spray Coatings and Sars-Cov-2 Surface Inactivation. *MRS Adv.* **2020**, *5*, 2873−2880.
(29) Hosseini, M.; Behzadinasab, S.; Chin, A. W.; Poon, L. L.; Ducker, W. A. Reduction of Infectivity of Sars-Cov-2 by Zinc Oxide Coatings. *ACS Biomater. Sci. Eng.* **2021**, *7*, 5022−5027, DOI: 10.1021/acsbiomaterials.1c01076.
(30) Cloutier, M.; Mantovani, D.; Rosei, F. Antibacterial Coatings: Challenges, Perspectives, and Opportunities. *Trends Biotechnol.* **2015**, *33*, 637−652.
(31) Salwiczek, M.; Qu, Y.; Gardiner, J.; Strugnell, R. A.; Lithgow, T.; McLean, K. M.; Thissen, H. Emerging Rules for Effective Antimicrobial Coatings. *Trends Biotechnol.* **2014**, *32*, 82−90.
(32) Rakowska, P. D.; Tiddia, M.; Faruqui, N.; Bankier, C.; Pei, Y.; Pollard, A. J.; Zhang, J.; Gilmore, I. S. Antiviral Surfaces and Coatings and Their Mechanisms of Action. *Commun. Mat.* **2021**, *2*, 53.
(33) Hosseini, M.; Behzadinasab, S.; Benmamoun, Z.; Ducker, W. A. The Viability of Sars-Cov-2 on Solid Surfaces. *Curr. Opin. Colloid Interface Sci.* **2021**, *55*, 101481.
(34) Singha, P.; Locklin, J.; Handa, H. A Review of the Recent Advances in Antimicrobial Coatings for Urinary Catheters. *Acta Biomater.* **2017**, *50*, 20−40.
(35) Sunada, K.; Minoshima, M.; Hashimoto, K. Highly Efficient Antiviral and Antibacterial Activities of Solid-State Cuprous Compounds. *J. Hazard. Mater.* **2012**, *235-236*, 265−270.
(36) Aydin Sevinç, B.; Hanley, L. Antibacterial Activity of Dental Composites Containing Zinc Oxide Nanoparticles. *J. Biomed. Mater. Res. B Appl. Biomater.* **2010**, *94*, 22−31.
(37) Pasquet, J.; Chevalier, Y.; Pelletier, J.; Couval, E.; Bouvier, D.; Bolzinger, M.-A. The Contribution of Zinc Ions to the Antimicrobial Activity of Zinc Oxide. *Colloids Surf., A* **2014**, *457*, 263−274.
(38) Young, M.; Ozcan, A.; Myers, M. E.; Johnson, E. G.; Graham, J. H.; Santra, S. Multimodal Generally Recognized as Safe Zno/Nanocopper Composite: A Novel Antimicrobial Material for the Management of Citrus Phytopathogens. *J. Agric. Food Chem.* **2017**, *66*, 6604−6608.
(39) M.El Saeed, A.; Abd El-Fattah, M.; Azzam, A. M.; Dardir, M. M.; Bader, M. M. Synthesis of Cuprous Oxide Epoxy Nanocomposite as an Environmentally Antimicrobial Coating. *Int. J. Biol. Macromol.* **2016**, *89*, 190−197.
(40) Akiyama, T.; Miyamoto, H.; Yonekura, Y.; Tsukamoto, M.; Ando, Y.; Noda, I.; Sonohata, M.; Mawatari, M. Silver oxide-containing hydroxyapatite coating has in vivo antibacterial activity in the rat tibia. *J. Orthop. Res.* **2013**, *31*, 1195−1200.
(41) Johnson, J. R.; Roberts, P. L.; Olsen, R. J.; Moyer, K. A.; Stamm, W. E. Prevention of Catheter-Associated Urinary Tract Infection with a Silver Oxide-Coated Urinary Catheter: Clinical and Microbiologic Correlates. *J. Infect. Dis.* **1990**, *162*, 1145−1150.
(42) Reddy, S. T.; Chung, K. K.; McDaniel, C. J.; Darouiche, R. O.; Landman, J.; Brennan, A. B. Micropatterned Surfaces for Reducing the Risk of Catheter-Associated Urinary Tract Infection: AnIn VitroStudy on the Effect of Sharklet Micropatterned Surfaces to Inhibit Bacterial Colonization and Migration of UropathogenicE-scherichia coli. *J. Endourol.* **2011**, *25*, 1547−1552.
(43) Ivanova, E. P.; Hasan, J.; Webb, H. K.; Truong, V. K.; Watson, G. S.; Watson, J. A.; Baulin, V. A.; Pogodin, S.; Wang, J. Y.; Tobin, M. J.; Löbbe, C.; Crawford, R. J. Natural Bactericidal Surfaces: Mechanical Rupture of Pseudomonas Aeruginosa Cells by Cicada Wings. *Small* **2012**, *8*, 2489−2494.
(44) Hasan, J.; Xu, Y.; Yarlagadda, T.; Schuetz, M.; Spann, K.; Yarlagadda, P. K. Antiviral and Antibacterial Nanostructured Surfaces with Excellent Mechanical Properties for Hospital Applications. *ACS Biomater. Sci. Eng.* **2020**, *6*, 3608−3618.
(45) Hewawaduge, C.; Senevirathne, A.; Jawalagatti, V.; Kim, J. W.; Lee, J. H. Copper-Impregnated Three-Layer Mask Efficiently Inactivates Sars-Cov2. *Environ. Res.* **2021**, *196*, 110947.
(46) Babar, S.; Weaver, J. H. Optical Constants of Cu, Ag, and Au Revisited. *Appl. Opt.* **2015**, *54*, 477−481.
(47) Lee, H.; Dellatore, S. M.; Miller, W. M.; Messersmith, P. B. Mussel-Inspired Surface Chemistry for Multifunctional Coatings. *Science* **2007**, *318*, 426−430.
(48) Ryu, J. H.; Messersmith, P. B.; Lee, H. Polydopamine Surface Chemistry: A Decade of Discovery. *ACS Appl. Mater. Interfaces* **2018**, *10*, 7523−7540.
(49) Platzman, I.; Brener, R.; Haick, H.; Tannenbaum, R. Oxidation of Polycrystalline Copper Thin Films at Ambient Conditions. *J. Phys. Chem. C* **2008**, *112*, 1101−1108.
(50) Park, J.-H.; Natesan, K. Oxidation of Copper and Electronic Transport in Copper Oxides. *Oxid. Met.* **1993**, *39*, 411−435.
(51) Zhao, L.; Chen, D.; Hu, W. Patterning of Metal Films on Arbitrary Substrates by Using Polydopamine as a Uv-Sensitive Catalytic Layer for Electroless Deposition. *Langmuir* **2016**, *32*, 5285−5290.
(52) Wang, K.; Dong, Y.; Zhang, W.; Zhang, S.; Li, J. Preparation of Stable Superhydrophobic Coatings on Wood Substrate Surfaces Via Mussel-Inspired Polydopamine and Electroless Deposition Methods. *Polymers* **2017**, *9*, 218.
(53) Frick, C. P.; Merkel, D. R.; Laursen, C. M.; Brinckmann, S. A.; Yakacki, C. M. Copper-Coated Liquid-Crystalline Elastomer via Bioinspired Polydopamine Adhesion and Electroless Deposition. *Macromol. Rapid Commun.* **2016**, *37*, 1912−1917.
(54) Gonzalez-Martinez, E.; Saem, S.; Beganovic, N. E.; Moran-Mirabal, J. Fabrication of Microstructured Electrodes Via Electroless Metal Deposition onto Polydopamine-Coated Polystyrene Substrates and Thermal Shrinking. *Nano Sel.* **2021**, *2*, 1926.
(55) Environmental Protection Agency Protocol for the Evaluation of Bactericidal Activity of Hard, Non-Porous Copper Containing Surface Products. https://www.epa.gov/sites/production/files/2016-02/documents/copper_and_copper-alloy_surface_protocol_revised_012916.pdf (accessed June 2, 2021).
(56) Bleichert, P.; Espírito Santo, C.; Hanczaruk, M.; Meyer, H.; Grass, G. Inactivation of Bacterial and Viral Biothreat Agents on Metallic Copper Surfaces. *BioMetals* **2014**, *27*, 1179−1189.
(57) Palmer, D. A.; Bénézeth, P.; Simonson, J. *Solubility of Copper Oxides in Water and Steam, 14th International Conference on the Properties of Water and Steam in Kyoto*, 2004; pp 491−496.

(58) Edwards, M.; Powers, K.; Hidmi, L.; Schock, M. R. The Role of Pipe Ageing in Copper Corrosion by-Product Release. *Water Sci. Technol.: Water Supply* **2001**, *1*, 25−32.
(59) Rifkind, J. M.; Shin, Y. A.; Heim, J. M.; Eichhorn, G. L. Cooperative disordering of single-stranded polynucleotides through copper crosslinking. *Biopolymers* **1976**, *15*, 1879−1902.
(60) Warnes, S. L.; Keevil, C. W. Inactivation of Norovirus on Dry Copper Alloy Surfaces. *PLoS One* **2013**, *8*, No. e75017.
(61) Liu, Y.; Ai, K.; Liu, J.; Deng, M.; He, Y.; Lu, L. Dopamine-Melanin Colloidal Nanospheres: An Efficient Near-Infrared Photothermal Therapeutic Agent for In Vivo Cancer Therapy. *Adv. Mater.* **2013**, *25*, 1353−1359.
(62) Environmental Protection Agency Reregistration Eligibility Decision (Red) for Coppers. https://www3.epa.gov/pesticides/chem_search/reg_actions/reregistration/red_G-26_26-May-09.pdf (accessed June 2, 2021).
(63) Zhou, P.; Deng, Y.; Lyu, B.; Zhang, R.; Zhang, H.; Ma, H.; Lyu, Y.; Wei, S. Rapidly-Deposited Polydopamine Coating Via High Temperature and Vigorous Stirring: Formation, Characterization and Biofunctional Evaluation. *PLoS One* **2014**, *9*, No. e113087.
(64) Chan, K. H.; Lai, S. T.; Poon, L. L. M.; Guan, Y.; Yuen, K. Y.; Peiris, J. S. M. Analytical Sensitivity of Rapid Influenza Antigen Detection Tests for Swine-Origin Influenza Virus (H1n1). *J. Clin. Virol.* **2009**, *45*, 205−207.
(65) Malenovska, H. Virus quantitation by transmission electron microscopy, TCID50, and the role of timing virus harvesting: A case study of three animal viruses. *J. Virol. Methods* **2013**, *191*, 136−140.

https://doi.org/10.1021/acsami.1c15505
ACS Appl. Mater. Interfaces 2021, 13, 54706−54714